Modulatory activity of ADNP on the hypoxia-induced angiogenic process in glioblastoma

AGATA GRAZIA D'AMICO[1*], GRAZIA MAUGERI[2*], BENEDETTA MAGRÌ[2], SALVATORE GIUNTA[2], SALVATORE SACCONE[3], CONCETTA FEDERICO[3], ELISABETTA PRICOCO[2], GIUSEPPE BROGGI[4], ROSARIO CALTABIANO[4], GIUSEPPE MUSUMECI[2,5], DORA REGLODI[6] and VELIA D'AGATA[2]

[1]Department of Drug and Health Sciences, University of Catania, I-95125 Catania; [2]Department of Biomedical and Biotechnological Sciences, Section of Anatomy, Histology and Movement Sciences, University of Catania, I-95100 Catania; [3]Department of Biological, Geological and Environmental Sciences, Section of Animal Biology, University of Catania; [4]Department of Medical and Surgical Sciences and Advanced Technologies 'G.F. Ingrassia', Anatomic Pathology, University of Catania, I-95123 Catania; [5]Research Center on Motor Activities (CRAM), University of Catania, I-95100 Catania, Italy; [6]Department of Anatomy, MTA-PTE PACAP Research Group, University of Pécs Medical School, 7622 Pécs, Hungary

Received March 22, 2022; Accepted June 22, 2022

DOI: 10.3892/ijo.2022.5462

Abstract. Glioblastoma multiforme (GBM) is a brain cancer with a poor prognosis that affects adults. This is a solid tumor characterized by a high rate of cell migration and invasion. The uncontrolled cell proliferation creates hypoxic niches in the tumor mass, which leads to the overexpression of hypoxia-inducible factors (HIFs). This induces the activation of the vascular endothelial growth factor (VEGF), which is responsible for uncontrolled neoangiogenesis. Recent studies have demonstrated the anti-invasive effect of pituitary adenylate cyclase-activating peptide (PACAP) in GBM. PACAP effects on the central nervous system are also mediated through the activity-dependent neuroprotective protein (ADNP) activation. To date, no evidence exists regarding its role in GBM. Therefore, the ADNP involvement in GBM was investigated. By analyzing ADNP expression in a human GBM sample through confocal microscopy, a high ADNP immunoreactivity was detected in most glial cells and its predominant expression in hypoxic areas overexpressing HIF-1α was highlighted. To investigate the role of ADNP on the HIF-VEGF axis in GBM, a human U87MG GBM cell line was cultured with a hypoxic mimetic agent, deferoxamine, and cells were treated with the smallest active fragment of ADNP, known as NAP. The protein expression and distribution of HIF-1α and VEGF was detected using western blot analysis and immunofluorescence assay. Results demonstrated that ADNP modulates the hypoxic-angiogenic pathway in GBM cells by reducing VEGF secretion, detected through ELISA assay, as well as modulating their migration, assessed through wound healing assay. Although deeper investigation is necessary, the present study suggested that ADNP could be involved in PACAP anti-invasive effects in GBM.

Correspondence to: Professor Velia D'Agata, Department of Biomedical and Biotechnological Sciences, Section of Anatomy, Histology and Movement Sciences, University of Catania, 87 Santa Sofia Road, I-95100 Catania, Italy
E-mail: vdagata@unict.it

*Contributed equally

Key words: glioblastoma multiforme, activity-dependent neuroprotective protein, hypoxia, angiogenesis, vascular endothelial growth factor

Introduction

Glioblastoma (GBM), known as grade IV astrocytoma, is a fatal brain cancer affecting adults with a median survival between 14-17 months (1). In a recent review, the existing criteria used for its classification were summarized based on histologic features (astrocytoma of grades I, II, III and IV, named as GBM), molecular subtypes (Proneural/Neural, Classical, and Mesenchymal), or gene mutations such as TP53, PTEN, Neu-rofibromin-1 and epidermal growth factor receptor (EGFR) or isocitrate dehydrogenase (IDH) enzyme mutations (2). This solid tumor is characterized by a stroma containing cells with a different phenotype, blood vessels and infiltrating cells, which confer epigenetic and genetic heterogeneity to the mass. This is directly responsible for the cancer progression and results in a difficult therapeutic approach (3).

Hypoxic niches are a common feature of solid tumors. In these areas, hypoxia triggers aberrant angiogenesis and promotes stem cell population growth in the cancer mass. These hypoxia-driven events are related to a poor prognosis as well as therapy resistance in patients with GBM (4,5). More specifically, the hypoxic microenvironment induces a transcription of hypoxia-inducible factors (HIFs), such as HIF-1α,

that translocases into the nucleus and binds to the constitutive HIF-1β subunit, forming a heterodimeric complex. This complex activates the hypoxia response elements, triggering the activation of numerous downstream target genes such as vascular endothelial growth factor (VEGF), which is involved in the neoangiogenesis process (6,7). Thus, the identification of molecules targeting the tumor hypoxic pathway could improve GBM regression. At present, the standard therapy consists of a multimodal approach including surgery, radiotherapy and chemotherapy with Temozolomide (TMZ) (8,9). This latter is a DNA alkylating agent, which induces the destruction of cancer cells by blocking DNA replication (10). However, TMZ has shown different side effects including hepatic impairment and myelosuppression (11).

Previously, it has been demonstrated that the pituitary adenylate cyclase-activating polypeptide (PACAP) is involved in GBM malignancy. It regulates cell invasion and interferes with epithelial-mesenchymal transition (EMT), a process implicated in invasiveness of cancer cells towards surrounding tissue (12-14). This peptide is expressed both in the central nervous system (CNS) and in peripheral organs where PACAP exerts numerous biological effects depending on the physio-pathological conditions (15-21). The multitude of PACAP effects depends on its binding to the G protein-coupled receptors known as PAC1 (PAC1-R), VPAC-1, and VPAC-2 receptors (VPAC1-R and VPAC2-R), through which it activates the adenylate cyclase (AC) and/or phospholipase C pathways (22). PACAP effects in the CNS are also mediated by the induction of the activity-dependent neuroprotective protein (ADNP), an intracellular astrocyte-derived neurotrophic factor (23-25). ADNP intracellular stimulation occurs in a bimodal manner based on PACAP concentration (26-28). In fact, sub-picomolar concentrations of PACAP induce ADNP release via PAC1-R activation, whereas nanomolar concentrations induce ADNP expression mediated through VPAC1-R stimulation (29-31). ADNP is a protein essential for brain development and cognitive activity (32,33). Furthermore, its involvement in different tumors such as malignant peripheral nerve sheath tumors (34), colon (35), breast (36), ovarian (37) and bladder cancer (38) and high-grade serous carcinoma (39) has been previously reported. However, the functional role of ADNP in other human cancer development remains poorly characterized, and no evidence exists regarding its involvement in GBM. In the present study, the ADNP involvement in this malignancy was investigated for the first time, in particular its role in tumor hypoxic areas. The results revealed that ADNP is expressed in most glial cells of human GBM sections, particularly in hypoxic areas. To investigate whether ADNP interferes with hypoxia-mediated aberrant angiogenesis, human GBM cells were exposed to a hypoxic mimetic agent, deferoxamine (DFX), and were treated with the smallest active element of ADNP, known as NAP. It is an 8-amino acid peptide synthesized from ADNP and contains its neuroprotective active site. NAP is largely used in different *in vitro* and *in vivo* studies showing protective activity already at femtomolar concentrations (40). Moreover, its chemical structure allows it to cross the cell membrane where it binds to microtubules and protects astrocytes and neurons (41,42). The present results suggested that ADNP exerts modulatory activity in GBM progression.

Materials and methods

Human GBM sample and cell lines. The frozen sections of one human GBM sample were provided from Anatomic Pathology, Department of Medical and Surgical Sciences and Advanced Technologies 'G.F. Ingrassia', University of Catania. The present study was approved (approval no. CRAM-015-2020; 16 March 2020) by the ethics committee of the Research Center on Motor Activities (CRAM) of the University of Catania (Catania, Italy). The single GBM sample was processed after the patient (female; 61 years-old; date of sample collection, 25/04/14) had signed the informed consent. The surgical sample was submitted for frozen sections at the Anatomic Pathology Laboratory from our Institution and the following inclusion criteria were adopted: i) representative and viable tumor tissue had to be present; ii) it must not have contained neither necrosis nor extensive hemorrhagic changes; and iii) the frozen tissue had to be sufficient to obtain additional sections for immunohistochemical and immunofluorescence analyses.

Further analyses were also performed by using human GBM cell lines of unknown origins, U87MG (cat. no. HTB-14) and A172 (cat. no. CRL-1620), obtained from the American Type Culture Collection (ATCC). These cell lines were cultured in Dulbecco's modified Eagle's medium (DMEM) with 10% of heat-inactivated fetal bovine serum (FBS), 100 U/ml penicillin and 100 μg/ml streptomycin (all from Sigma-Aldrich; Merck KGaA) and incubated at 37˚C in a humidified atmosphere with 5% CO_2 as previously described (43). DFX (100 μM; Sigma-Aldrich; Merck KGaA) was used to mimic hypoxic conditions. In particular, U87MG cells were cultured for 24 h in normoxia or DFX-induced hypoxia with or without NAP (New England Peptide, Inc.) at different concentrations of 10 nM, 100 nM and 1 μM. The use of exogenous administration of DFX, representing a hypoxia-mimetic iron chelator, offers the advantage of allowing the experimenter to open the culture plate or dish numerous times without altering the hypoxic conditions respect to the cell incubation method in the hypoxic chamber.

Immunohistochemical assay. One surgically resected tumor sample was included in OCT and fresh-frozen sections were cut at 5 μM and fixed in 4% paraformaldehyde for 30 min at room temperature. Subsequently, the inhibition of the endogenous peroxidase activity was performed as previously described (44) by using 3% H_2O_2 in methanol for 10 min. The sections were then incubated with 1% bovine serum albumin (BSA) (cat. no. A-3294; Sigma-Aldrich; Merck KGaA) in PBS for 1 h at room temperature in order to reduce non-specific staining. Subsequently, they were incubated overnight at 4˚C with rabbit anti-ADNP primary antibody (1:50; cat. no. NBP1-89236; Novus Biologicals, LLC). Then, the sections were incubated at 4˚C for 30 min with secondary antibodies conjugated to polymer-HRP (LSAB+ System-HRP; cat. no. K0609; Dako; Agilent Technologies, Inc.). The immunoreaction was revealed by incubating at room temperature the sections for 5 min with the 3,3'-diaminobenzidine (DAB) solution (DAB substrate kit; cat. no. SK-4100; Vector Laboratories, Inc.). The sections were incubated for 3 min at room temperature with hematoxylin that was used as a nuclear counterstain. The stained sections were dehydrated through graded alcohol, cleared in xylene

and covered with neutral balsam. The sections were examined with a Zeiss Axioplan light microscope (Carl Zeiss AG) and images were captured with a digital camera (AxioCam MRc5; Carl Zeiss AG).

Immunofluorescence assay. To determine the distribution of ADNP, GFAP, and HIF-1α, immunofluorescence analysis was performed as previously described (45). One surgically resected tumor sample was included in OCT and fresh-frozen sections were cut at 5 μM and fixed in 4% paraformaldehyde for 30 min. Subsequently, the inhibition of the endogenous peroxidase activity was performed as previously described (44), by using 3% H_2O_2 in methanol for 10 min. The sections were then incubated with 1% BSA dissolved in PBS for 1 h in order to reduce non-specific staining. They subsequently were incubated overnight with at 4˚C with rabbit anti-ADNP (1:50), mouse anti-HIF-1α (1:50; cat. no. NB100-105; Novus Biologicals, LLC) and mouse anti-GFAP (1:100; cat. no. IF03L, Calbiochem; Merck KGaA) antibody.

Cells were cultured on glass cover slips, fixed in 4% paraformaldehyde in PBS for 15 min at room temperature, permeabilized with 0.2% Triton X-100 (cat. no. sc-29112; Santa Cruz Biotechnology, Inc.), blocked with 0.1% BSA in PBS and then probed with rabbit anti-ADNP (1:50) and mouse anti-HIF-1α (1:50) antibody. Signals were revealed with Alexa Fluor 488-conjugated goat anti-rabbit (1:20,000; cat. no. A-11008) or Alexa Fluor 594-conjugated goat anti-mouse (1:30,000; cat. no. A-21203; both from Thermo Fisher Scientific, Inc.) secondary antibodies for 1 h at room temperature (shielded from light). DNA was counterstained with 4,6-diamidino-2-phenylindole (DAPI; cat. no. 940110; Vector Laboratories, Inc.). After a series of washes in PBS and double-distilled water, the fixed cells were cover-slipped with Vectashield mounting medium (Vector Laboratories, Inc.). Immunolocalization was analyzed by confocal laser scanning microscopy (Zeiss LSM700). Green and blue signals were respectively detected with laser light at 488 nm/10 mW and 405 nm/5 mW by using the objective 'PLANAPOCHROMAT' 63x/1,40 OIL DIC M27. Each scan was individually digitalized by a high sensitivity photomultiplier tube using the following acquisition setup: Gain master: 776; digital offset: -202; digital gain: 1.0. All acquisitions were performed with ZEN-2010 software (Zeiss GmbH).

Western blot analysis. Proteins were extracted with buffer containing 20 mM Tris (pH 7.4), 2 mM EDTA, 0.5 mM EGTA, 50 mM mercaptoethanol, 0.32 mM sucrose and a protease inhibitor cocktail (Roche Diagnostics) as previously described (43). The total cell lysates were homogenized, sonicated twice for 20 sec, and then protein concentrations were determined by the Quant-iT Protein Assay kit (cat. no. Q33211; Invitrogen; Thermo Fisher Scientific, Inc.). The protein homogenate (~35 μg) was diluted in Laemmli buffer (cat. no. 1610747; Bio-Rad Laboratories, Inc.), heated at 70˚C for 10 min, separated by electrophoresis by using 4-15% precast polyacrylamide gel Mini-PROTEAN TGX™ Precast Protein Gels (cat. no. 4561084) and subsequently transferred in nitrocellulose membrane (cat. no. 1704158; both from Bio-Rad Laboratories, Inc.). The Precision Plus Protein Standard (cat. no. 161-0373; Bio-Rad Laboratories, Inc.) was used to monitor electrophoresis. The proteins transferred onto nitrocellulose membrane were blocked for 1 h at room temperature with Odyssey Blocking Buffer (cat. no. 927-70001; LI-COR Biosciences), and incubated overnight at 4˚C with rabbit anti-ADNP (1:200), mouse anti-HIF-1α (1:200), goat polyclonal anti-VEGF (1:200; cat. no. sc-1836) and rabbit polyclonal anti-β-tubulin (cat. no. sc-9104; both from Santa Cruz Biotechnology, Inc.). The secondary antibodies [goat anti-rabbit IRDye 800CW (1:20,000; cat. no. 926-32211), donkey anti-goat IRDye 800CW (1:20,000; cat. no. 926-32214) and goat anti-mouse IRDye 680CW (1:30,000; cat. no. 926-68020D; all from LI-COR Biosciences)] were used. Blots were visualized with an Odyssey Infrared Imaging System (Odyssey; https://www.bioagilytix.com/li-cor-for-quantitative-western-blots/) and the densitometric analyses of blots were performed by using the ImageJ software version 1.46 (Nstional Institutes of Health). Values were normalized to β-tubulin that was used as a loading control.

ELISA. VEGF-A release in conditioned media was measured by using the ELISA sandwich enzymatic method with a specific anti-VEGF-A antibody (human VEGF-A; cat. no. ELH-VEGF; RayBiotech, Inc.) coated on a 96-well plate, according to the manufacturer's guidelines. Briefly, confluent U87MG cells cultured in media supplemented with 1% FBS were treated for 24 h with DFX with or without 100 nM NAP. Standards or supernatants from samples were pipetted into the wells containing the immobilized anti-VEGF-A antibody. Then, wells were washed before adding biotinylated anti-human VEGF antibody. Following incubation, the unbound biotinylated antibody was washed off, and HRP-conjugated streptavidin was pipetted in each well. After an additional wash step, a 3,3',5,5'-tetramethylbenzidine substrate solution was added to each well, resulting in a blue coloration proportional to the amount of bound VEGF. Finally, the stop solution was added, and the colorimetric intensity of the blue substrate now turned yellow was measured at 450 nm. The mean absorbance was calculated for each set of duplicate standards, controls and samples, and the average zero standard optical density was subtracted.

Conditioned medium (CM) preparation and tube formation assay. The U87MG cells were cultured in a medium containing 1% FBS, representing CM1 (control) or containing either 100 nM NAP (CM2) or 100 μM DFX (CM3) or DFX + 100 nM NAP (CM4). They were incubated for 24 h at 37˚C. Subsequently, the CMs were collected and after centrifugation at 15,000 x g for 5 min at room temperature the supernatants were frozen at -80˚C until use. By adding 95 μl of Geltrex matrix for each well in a plate of 24 wells for 30 min at 37˚C, polymerization was enabled. Murine micro-vascular endothelial cells (H5V) were cultured overnight in a starved medium. Therefore, the H5V were seeded into the layer of Geltrex matrix and cultured in a medium containing 200 μl of CM1, CM2, CM3 or CM4 at 37˚C for 24 h. A total of 5 randomly selected fields of view were captured with a digital camera (Canon) attached to a light inverted microscope (Axio Observer A1; Carl Zeiss AG). Tube number per field was calculated as percentage of control (%).

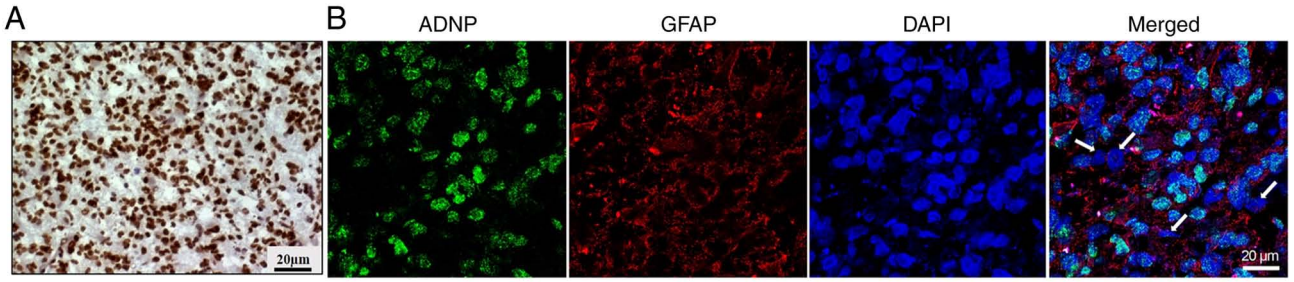

Figure 1. ADNP expression in human GBM sections. (A) Representative photomicrograph of ADNP immunoreactivity detected in a frozen GBM sample. (B) Photomicrographs reveal the immunofluorescent signal of ADNP and GFAP in a frozen GBM sample. White arrows indicate ADNP immune-negative cells. Scale bar, 20 μm. ADNP, activity-dependent neuroprotective protein; GBM, glioblastoma.

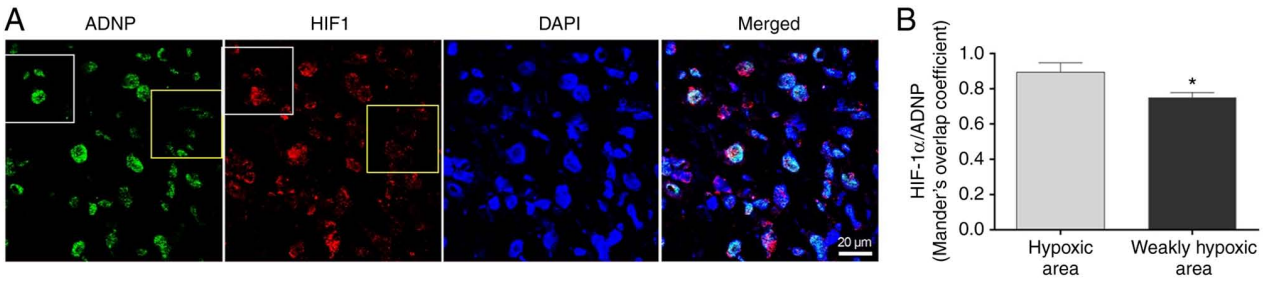

Figure 2. ADNP and HIF-1α co-localization in human GBM sections. (A) Photomicrographs show the immunofluorescence signal of ADNP (green) and HIF-1α expression (red) in fresh-frozen sections of a surgically resected GBM sample. Nuclei were stained with DAPI. The white squares indicate a representative hypoxic area with higher HIF-1α expression than the non-hypoxic area outlined by yellow squares with a weak HIF-1α expression. (B) HIF-1α/ADNP expression in these selected areas were analyzed by using Mander's overlap coefficient. Data represent the mean ± SEM. *P<0.05. ADNP, activity-dependent neuroprotective protein; HIF, hypoxia-inducible factor; GBM, glioblastoma.

Wound healing assay. U87MG cells were cultured in a six-well plate at a density of $5x10^4$ cells/well, then were scratched with a 200 μl pipette tip and wound closure was followed. Cells were incubated in a 1%-FBS medium with or without 100 nM NAP either in normoxia or in DFX-induced hypoxia (DFX 100 μM) and the distance that the advancing cells had moved into the cell-free (wound) area was measured after 24 h. Quantitative measurement of the wound area was performed under a light inverted microscope and calculated using ImageJ software version 1.46 (National Institutes of Health). Data are represented as % wound closure measured 24 h after scratching, observed in two random fields per well, in duplicate wells and expressed as a percentage respect to control (%).

Statistical analysis. To analyze the results, GraphPad Prism version 6 software (GraphPad Software, Inc.) was used and data are represented as the mean ± standard error of the mean (SEM). An unpaired, two-tailed Student's t-test was performed for comparisons between two groups. One-way analysis of variance was used to compare differences among three or more groups. Statistical significance was determined with the Tukey-Kramer post hoc test. Co-localization of ADNP with HIF-1α was analyzed using Mander's overlap coefficient and unpaired t-tests. The level of significance for all statistical tests was set at $P \leq 0.05$.

Results

ADNP expression in GBM tissue and cells. ADNP expression was detected in a GBM sample by immunohistochemical analysis (Fig. 1A). The analyzed GBM was classified as IDH-wild-type tumors obtained from the original tumor of one patient. Since the cancer tissue is characterized by high cellular heterogeneity (46-48), to clarify in an improved way the phenotype of the cells expressing ADNP, double-labeling staining was conducted by using the selected marker for ADNP with that against GFAP. As revealed in Fig. 1B, most of the cells were immune-positive to both GFAP (red fluorescence) and ADNP (green fluorescence). To investigate the ADNP expression in the hypoxic areas of GBM, its tissue co-expression with HIF-1α was detected by performing double-immunofluorescence analysis on human GBM sections (Fig. 2A). The white square indicate the hypoxic area displaying enhanced levels of HIF-1α and the yellow square to include the non-hypoxic area (Fig. 2A). The immunofluorescence signals detected for ADNP in hypoxic areas were quantified through the Mander's overlap coefficient. It was revealed that ADNP expression was significantly reduced in weakly hypoxic areas compared with hypoxic areas (Fig. 2B; $P<0.05$).

To characterize the ADNP role in this tumor, further experiments were carried out *in vitro* by using A172 and U87MG GBM cell lines. By performing western blot analysis, a similar protein expression profile was observed between GBM tissue and U87MG cells. By contrast, no signal was detected in A172 cells (Fig. 3A and B). This data was corroborated by immunofluorescence analysis revealing an ADNP immune-positive signal in the U87MG cells both in nuclear and in cytoplasmic compartments (Fig. 3C), in contrast to very low immunoreactivity detected in A172 cells. This evidence suggested that peptide expression depends on cell genotype (49).

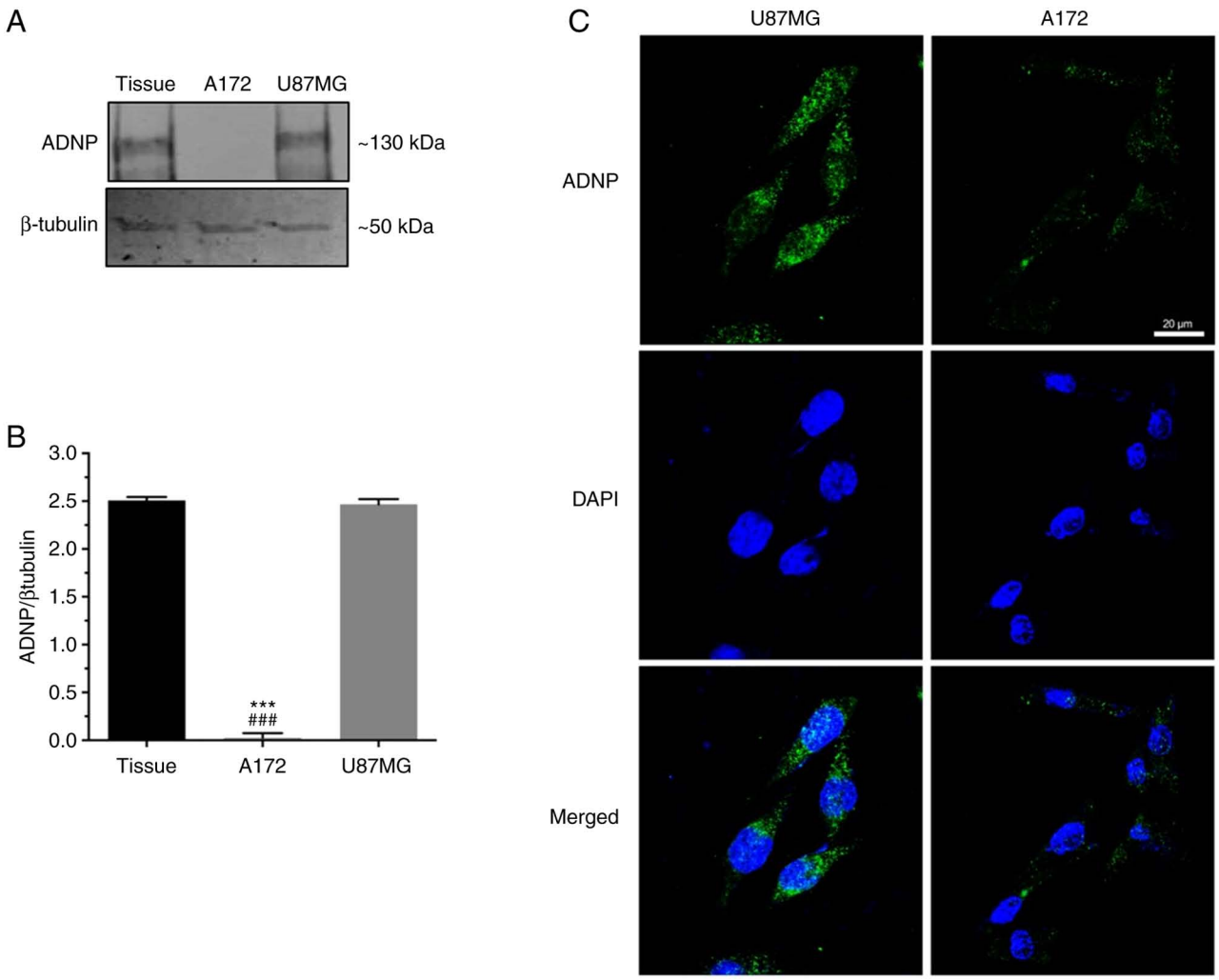

Figure 3. ADNP expression in a frozen GBM sample and in A172 and U87MG GBM cell lines. (A) Representative immunoblots of ADNP expression in one frozen GBM sample, A172 and U87MG cell homogenates. (B) The bar graphs show quantitative analysis of signals obtained by three independent experiments. Data are presented as the mean ± SEM. (C) The photomicrographs show the distribution of ADNP (green fluorescence) in A172 and U87MG cell lines. Scale bar, 20 μm. ***P<0.001 vs. Frozen sample and $^{###}$P<0.01 vs. U87MG, as determined by one-way ANOVA followed by Tukey's post-hoc test. ADNP, activity-dependent neuroprotective protein; GBM, glioblastoma.

Role of ADNP on the hypoxic angiogenic pathway. Due to the important role of the hypoxic microenvironment on tumor progression, it was investigated whether hypoxic insult affects ADNP expression in U87MG and A172 cells. In a preliminary study, the HIF-1α expression at different time points after DFX treatment was analyzed to verify the hypoxia status. Based on the results, 24 h was selected as a time point, as in this time frame the HIF-1α levels were higher than levels of the other examined time points of 12, 24 and 48 h (data not shown). As revealed in Fig. 4A and B, DFX treatment significantly increased ADNP expression compared with untreated U87MG cells (**P<0.01 vs. Control). By contrast, A172 cells did not express ADNP either in basal conditions or after DFX treatment (Fig. 4D). Based on this evidence, U87MG were selected cells to conduct further experiments. The detection of HIF-1α levels was used as a positive control to confirm that hypoxia occurs (Fig. 4C and E; ***P<0.001 vs. Control). To understand the role of ADNP on hypoxia-induced GBM progression in an improved way, the effect of NAP, the active fragment of ADNP, was analyzed at different concentrations in U87MG cell line cultured in DFX. As demonstrated in Fig. 5, 100 nM NAP represents the lower concentration that significantly affected HIF-1α levels by reducing its expression as compared with DXF-treated cells ($^{###}$P<0.01 vs. DFX). Based on this result, 100 nM of NAP was used to study the role of ADNP on the hypoxic/angiogenic pathway in U87MG cells. DFX-induced hypoxia significantly increased HIF-1α levels in respect to the control group (Fig. 6A and B; ***P<0.001 vs. Control). Exogenous administration of the peptide significantly reduced HIF-1α expression in DFX-treated cells (Fig. 6A and B; $^{###}$P<0.01 vs. DFX). This data was corroborated by immunofluorescence analysis (Fig. 6D) since the high HIF-1α immunoreactivity displayed in the DFX-treated group was downregulated following NAP exogenous administration. To characterize the effect of NAP on the hypoxia-angiogenic pathway, VEGF expression and release were measured in human GBM cells cultured for 24 h in a medium containing DFX. Data revealed increased intracellular VEGF levels (Fig. 6A) as well as its secretion (Table I) in the DFX-treated group compared with control cells (**P<0.001 vs. Control; Fig. 6C). NAP treatment significantly reduced VEGF expression (Fig. 6C) and release (Table I) in the culture medium of cells grown under

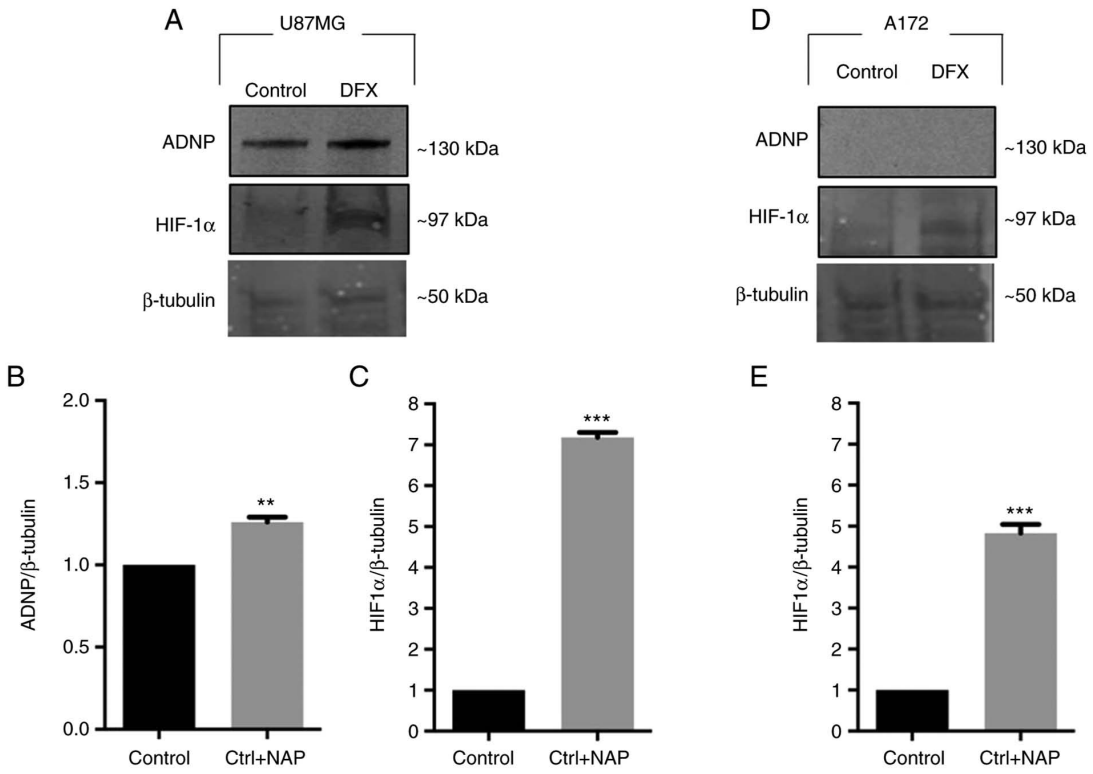

Figure 4. ADNP and HIF-1α expression in U87MG and A172 cells cultured in DFX-induced hypoxia. (A and D) Representative immunoblots of ADNP and HIF-1α expression in (A) U87MG and (D) A172 cells cultured in normoxia (Control) and in DFX-induced hypoxia (DFX). (B, C and E) The bar graphs show quantitative analysis of signals obtained by three independent experiments. In the bar graph, values are expressed as the mean ± SEM by setting the control group value to 1. **P<0.01 and ***P<0.001 vs. Control, as determined by unpaired two-tailed Student's t-test. ADNP, activity-dependent neuroprotective protein; HIF, hypoxia-inducible factor; DFX, deferoxamine.

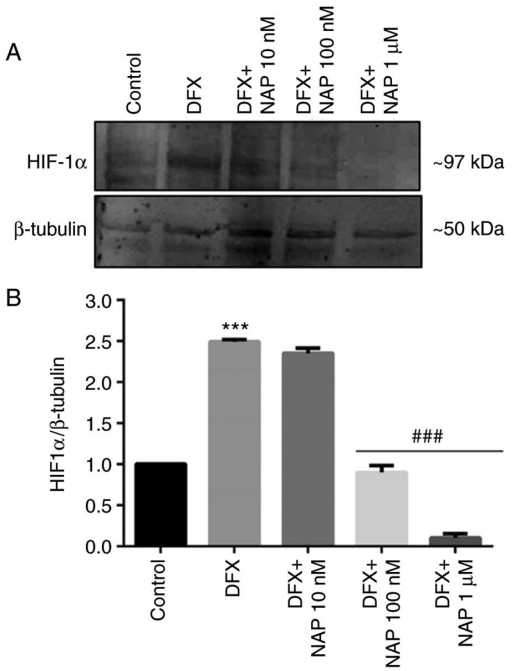

Figure 5. Dose response effect of NAP on HIF-1α expression cultured in DFX for 24 h. (A) Representative immunoblots of HIF-1α expression in U87MG cells treated with vehicle (Control), DFX and DFX plus NAP at 10 nM, 100 nM and 1 μM for 24 h. (B) The bar graphs show quantitative analysis of signals obtained by three independent experiments. In the bar graph, values are expressed as the mean ± SEM by setting the control group value to 1. ***P<0.001 vs. Control and $^{###}$P<0.001 vs. DFX, as determined by one-way ANOVA followed by Tukey's post-hoc test. HIF, hypoxia-inducible factor; DFX, deferoxamine.

normoxia or DFX-induced hypoxia (***P<0.001 vs. Control; $^{###}$P<0.001 vs. DFX).

To further analyze the involvement of NAP in the angiogenesis process, the number of tube-like structures formed by H5V microvascular endothelial cells cultured in a CM derived from U87MG cells cultured under normoxia or DFX-induced hypoxia and treated with NAP was measured. The results revealed that the number of tube-like structures was increased in cells cultured in CM3, derived from GBM cells exposed to DFX and containing 6,427 pg/ml VEGF, as compared with CM1 cultured cells containing 3784 pg/ml VEGF (Fig. 7A and B; ***P<0.001 vs. CM1). The number of new vessels was significantly reduced in H5V cells cultured in CM4, deriving from DFX + NAP-treated U87MG cells and containing 2,622 pg/ml VEGF (Fig. 7A and B; $^{###}$P<0.001 vs. CM3). The aforementioned data confirmed that NAP interferes with the angiogenic process by reducing new vessel formation.

Since hypoxia-driven tumor progression is strictly linked to an increased cell migration, a preliminary study was also conducted to characterize ADNP effect on invasion potential of GBM cells cultured under hypoxia. As revealed in Fig. S1, NAP treatment of DFX-exposed cells significantly decreased the percentage of wound closure as compared with DFX-treated group.

Discussion

Uncontrolled cell proliferation in GBM forms the hypoxic area which promotes aberrant angiogenesis and cancer stem

Table I. VEGF content in the CM deriving from U87MG cells. The VEGF levels were detected in supernatants and expressed in pg/ml. Data resulting from three independent experiments are represented as the mean ± SEM.

U87MG cell line-derived conditioned media	CM1 (Control) Mean + SEM	CM2 (Control + NAP) Mean + SEM	CM3 (DFX) Mean + SEM	CM4 (DFX + NAP) Mean + SEM
VEGF (pg/ml)	3,784±107	2,495±47[a]	6,427±108[a]	2,622±63[b]

[a]P<0.001 vs. Control and [b]P<0.001 vs. DFX, as determined by one-way ANOVA followed by Tukey's post-hoc test. VEGF, vascular endothelial growth factor; CM, conditioned medium; DFX, deferoxamine.

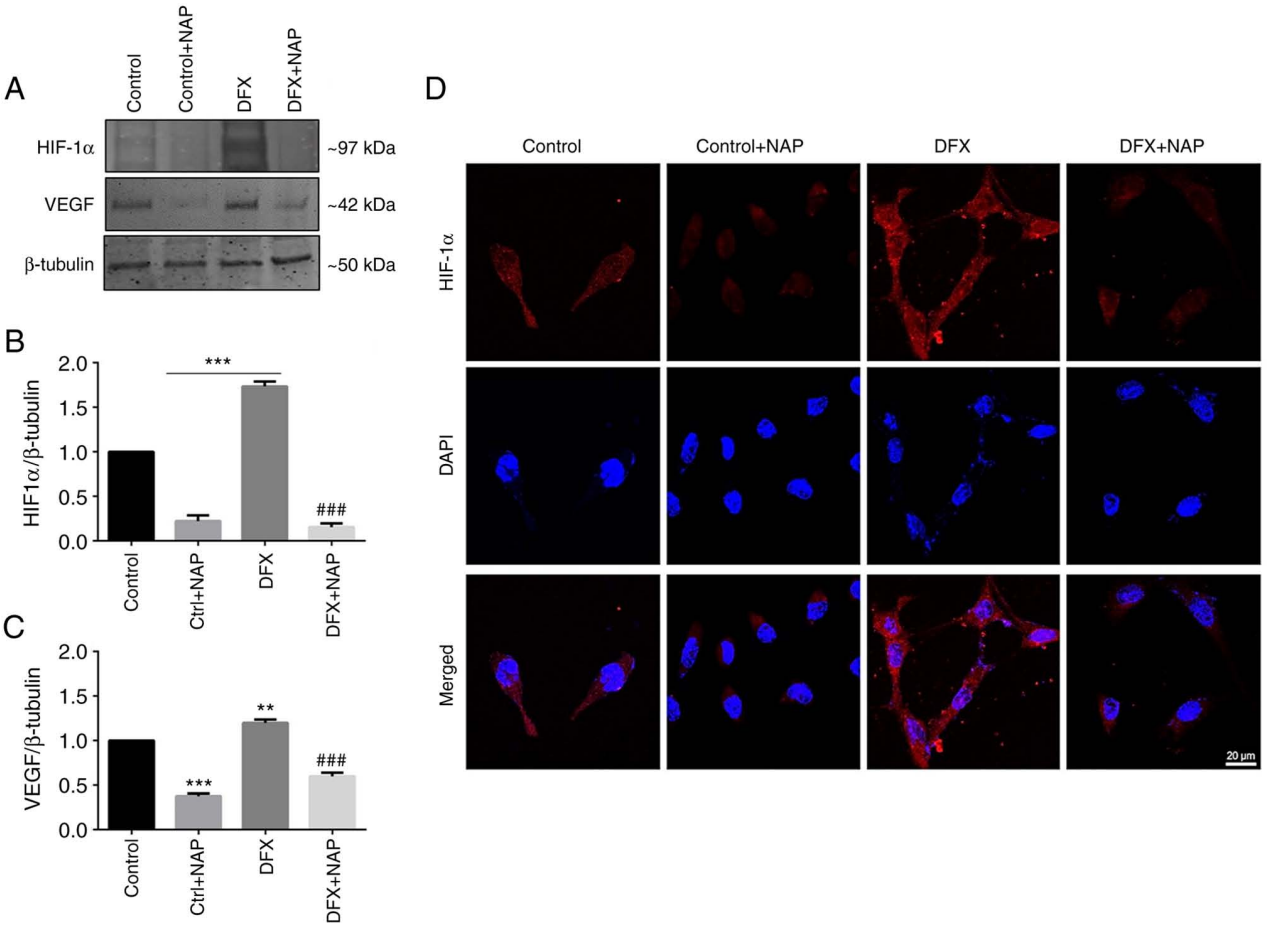

Figure 6. NAP modulates HIF-1α expression and localization and VEGF expression in U87MG cells cultured in DFX-induced hypoxia. (A) Representative immunoblots of HIF-1α and VEGF expression in U87MG treated with vehicle (Control), 100 nM of NAP (Control + NAP), DFX or DFX plus NAP (DFX + NAP) for 24 h. (B) The bar graphs show quantitative analysis of signals obtained by three independent experiments. In the bar graph, values are expressed as the mean ± SEM by setting the control group value to 1. (C) Photomicrographs demonstrate the immunofluorescence signal of HIF-1α expression (red fluorescence) in U87MG cells treated with 100 nM of NAP either normoxia or DFX-induced hypoxia. Scale bar, 20 μm. **P<0.001 or ***P<0.001 vs. Control and $^{###}$P<0.001 vs. DFX, as determined by one-way ANOVA followed by Tukey's post-hoc test. HIF, hypoxia-inducible factor; VEGF, vascular endothelial growth factor.

cell proliferation inside the tumor mass. Previous findings have highlighted the anti-invasive role exerted by PACAP in GBM (13,14,50,51). In addition to activation of its related receptors, this peptide also acts indirectly through intracellular stimulation of ADNP (23,30,31). The latter is implicated in brain development during embryogenesis. It has also been identified that its loss-of-function mutation is related to carcinogenesis (52-54). Previously, its involvement in various tumors has been demonstrated, even though its role remains controversial depending on the type of cancer. It acts as a tumor suppressor in triple-negative breast cancer (36), as oncogene in ovarian and bladder cancer (37,38) as well as onco-suppressor or oncogene in colorectal cancer (35). To date, no findings are available regarding ADNP implication in GBM. In particular, it was demonstrated in the present study that it is overexpressed in most glial cells of human GBM. This evidence is in consistency with previous studies reporting an increased ADNP expression in tumors (38,39). Its upregulation was associated with a poor prognosis in bladder cancer, where it prompted tumor growth through activation of

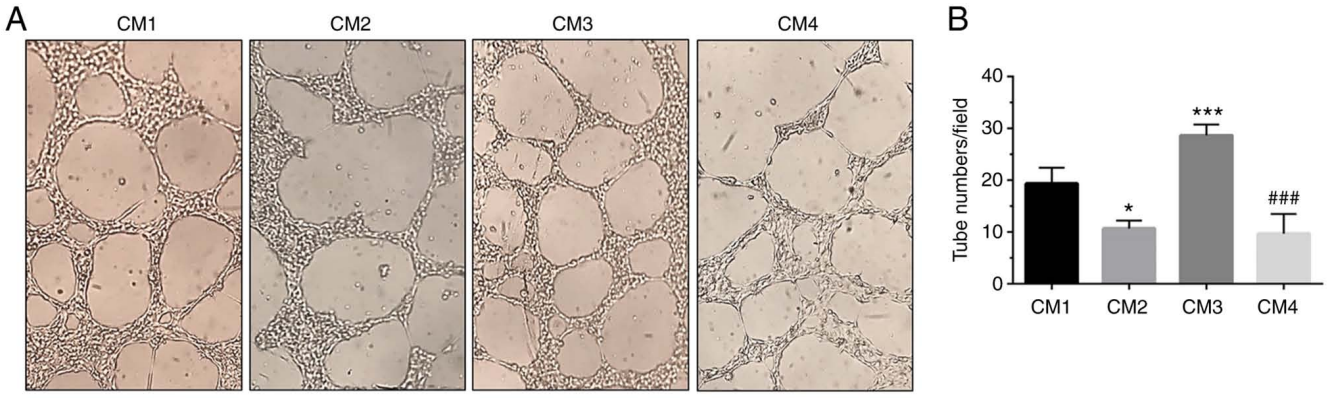

Figure 7. Effect of NAP on new vessel formation. (A) Microphotographs show tubes formed by H5V cells cultured in CM1, CM2, CM3 or CM4, respectively. (B) In the bar graph, the number of tubes/fields is expressed as the mean ± SEM. *P<0.05 or ***P<0.001 vs. CM1 (Control) and $^{###}$P<0.001 vs. CM3 (deferoxamine), as determined by one-way ANOVA followed by Tukey's post-hoc test. CM, conditioned medium.

AKT signaling and induced cisplatin resistance by promoting cancer cell migration and EMT (38,55). Furthermore, it is involved in the death resistance of malignant peripheral nerve sheath tumor cells (34). Notably, higher ADNP immunoreactivity was detected in the hypoxic area of the tumor mass by suggesting a direct relation between its upregulation and the hypoxic microenvironment. Specifically, the hypoxic niches are generated in the tumor when increased cell proliferation leads to growth of tissue mass, not supported by an adequate oxygen supply. These areas present tissue necrosis and aberrant neoangiogenesis sustained by activation of HIF-VEGF system. To understand the biological impact of ADNP overexpression in hypoxic niches of GBM, an *in vitro* study was performed by using U87MG GBM cells showing a similar protein expression pattern as compared with the human GBM sample. These cells exposed to DFX, mimicking microenvironmental hypoxia, overexpressed ADNP. This result could be attributed to their tumorigenic potential considering that ADNP overexpression was only revealed in this cell line whereas was undetectable in A172 cells. These results could be attributed to the different genotype of these cell lines. Consistently, U87MG overexpress nestin and vimentin, two markers of immature astroglia cells and malignancy, whereas the A172 cells are less tumorigenic since they do not express these markers (49).

To characterize the role of ADNP in the hypoxic niches of the tumor, its smallest active element, NAP owing a chemical structure allowing cell membrane penetration was used (26,52,53). Its protective effects are widely reported in literature, demonstrating its implication in numerous disorders (56,57). By treating DFX-exposed cells with NAP, it was demonstrated that ADNP interferes with tumor malignancy by downregulating hypoxia-VEGF pathway. In a previous study, it was demonstrated that cancer cells of hypoxic niches release numerous factors in the extracellular microenvironment such as VEGF that actively participates to aberrant angiogenesis (58). This biological process involves migration of endothelial cells toward the extracellular matrix, where they cooperate to create a new lumen (58). In the present study, it was demonstrated that cancer cells release VEGF in the extracellular medium, which triggers neovascularization process as revealed by increased formation of tube-like structures when H5V endothelial cells were cultured in CM derived from GBM cells exposed to DFX (CM3). CM derived from U87MG cells treated with NAP contains a reduced amount of VEGF which, in turn, it is related to a reduced formation of tube-like structures.

The preliminary study conducted is in line with previous evidence demonstrating that induction of ADNP expression in colon cancer leads to the inhibition of tumor growth, which was also correlated with prolonged survival of the animals (35). In the aforementioned type of cancer, ADNP acted as a negative regulator of WNT signaling, one of the main factors responsible for colon tumor development. Moreover, the silencing of ADNP increased cell proliferation and tumor progression in xenografts *in vivo*. It is worth noting that patients with high levels of ADNP survived during the follow-up period, while moderate or negative ADNP expression was related to a high frequency of cancer-related death. These data suggested that ADNP could be considered an onco-suppressor in colon cancer.

In a previous study, enhanced expression of PACAP and PAC1R was demonstrated in hypoxic areas of GBM (14). Based on the present results, it cannot be excluded that the aforementioned effects are mediated by PACAP binding to its receptor PAC1R which stimulates ADNP formation in the hypoxic niches of GBM. At the light of this aspect, it is planned to further characterize the role of PACAP-ADNP axis in GBM.

In conclusion, the present results suggested that ADNP may act as a tumor suppressor in GBM, in particular, in the hypoxic niches by interfering with the aberrant angiogenesis.

Acknowledgements

Not applicable.

Funding

The present study was supported by the STARTING GRANT 2020, titled 'Regulatory effect of PACAP-ADNP axis and its involvement in modulation of Glioblastoma multiforme', Department of Drug Science, University of Catania. The present study was also supported by National Research, Development and Innovation Fund (grant nos. K135457, TKP 2021-AGE-16 and ELKH-TKI-14016).

Availability of data and materials

All data generated or analyzed during this study are included in this published article.

Authors' contributions

AGD, GMa and VD conceptualized the study. BM, SG, GMu, SS and CF provided methodology. EP provided technical support. AGD and CF performed software analysis. AGD and GM conducted investigation. RC and GB provided resources. AGD and GMa performed data curation. AGD, GMa, DR and VD wrote the original draft. VD and DR wrote, reviewed and edited the manuscript. GMu, VD and DR supervised the study. AGD and DR acquired funding. AGD, GMa, BM, SG, SS and CF, EP, RC, GB, GMu, DR and VD made substantial contributions to conception and design of the present study, acquisition, analysis and interpretation of data. AGD, GMa, RC, GB, DR and VD were involved in drafting the manuscript or revising it critically for important intellectual content. AGD, GMa and VD confirm the authenticity of all the raw data. All authors have read and approved the final version of the manuscript.

Ethics approval and consent to participate

The present study was approved (approval no. CRAM-015-2020; 16 March 2020) by the ethics committee of the Research Center on Motor Activities (CRAM) of the University of Catania (Catania, Italy). Written informed consent was obtained from the subject involved in the present study.

Patient consent for publication

Not applicable.

Competing interests

The authors declare that they have no competing interests.

References

1. Wesseling P and Capper D: WHO 2016 classification of gliomas. Neuropathol Appl Neurobiol 44: 139-150, 2018.
2. D'Amico AG, Maugeri G, Vanella L, Pittalà V, Reglodi D and D'Agata V: Multimodal role of PACAP in glioblastoma. Brain Sci 11: 994, 2021.
3. Wenger A, Vega SF, Kling T, Bontell TO, Jakola AS and Carén H: Intratumor DNA methylation heterogeneity in glioblastoma: Implications for DNA methylation-based classification. Neuro Oncol 21: 616-627, 2019.
4. Semenza GL: Intratumoral hypoxia, radiation resistance, and HIF-1. Cancer Cell 5: 405-406, 2004.
5. Vaupel P and Mayer A: Hypoxia in cancer: Significance and impact on clinical outcome. Cancer Metastasis Rev 26: 225-239, 2007.
6. Maugeri G, D'Amico AG, Reitano R, Magro G, Cavallaro S, Salomone S and D'Agata V: PACAP and vip inhibit the invasiveness of glioblastoma cells exposed to hypoxia through the regulation of HIFs and EGFR expression. Front Pharmacol 7: 139, 2016.
7. Maugeri G, D'Amico AG, Rasà DM, Saccone S, Federico C, Cavallaro S and D'Agata V: PACAP and VIP regulate hypoxia-inducible factors in neuroblastoma cells exposed to hypoxia. Neuropeptides 69: 84-91, 2018.
8. Anjum K, Shagufta BI, Abbas SQ, Patel S, Khan I, Shah SAA, Akhter N and Hassan SSU: Current status and future therapeutic perspectives of glioblastoma multiforme (GBM) therapy: A review. Biomed Pharmacother 92: 681-689, 2017.
9. Touat M, Idbaih A, Sanson M and Ligon KL: Glioblastoma targeted therapy: Updated approaches from recent biological insights. Ann Oncol 28: 1457-1472, 2017.
10. Stupp R, Mason WP, van den Bent MJ, Weller M, Fisher B, Taphoorn MJ, Belanger K, Brandes AA, Marosi C, Bogdahn U, *et al*: Radiotherapy plus concomitant and adjuvant temozolomide for glioblastoma. N Engl J Med 352: 987-996, 2005.
11. Weller M, van den Bent M, Tonn JC, Stupp R, Preusser M, Cohen-Jonathan-Moyal E, Henriksson R, Rhun EL, Balana C, Chinot O, *et al*: European association for neuro-oncology (EANO) guideline on the diagnosis and treatment of adult astrocytic and oligodendroglial gliomas. Lancet Oncol 8: e315-e329, 2017.
12. Cochaud S, Chevrier L, Meunier AC, Brillet T, Chadéneau C and Muller JM: The vasoactive intestinal peptide-receptor system is involved in human glioblastoma cell migration. Neuropeptides 44: 373-383, 2010.
13. Cochaud S, Meunier AC, Monvoisin A, Bensalma S, Muller JM and Chadéneau C: Neuropeptides of the VIP family inhibit glioblastoma cell invasion. J Neurooncol 122: 63-73, 2015.
14. Maugeri G, D'Amico AG, Saccone S, Federico C, Rasà DM, Caltabiano R, Broggi G, Giunta S, Musumeci G and D'Agata V: Effect of PACAP on hypoxia-induced angiogenesis and epithelial-mesenchymal transition in glioblastoma. Biomedicines 9: 965, 2021.
15. Toth D, Szabo E, Tamas A, Juhasz T, Horvath G, Fabian E, Opper B, Szabo D, Maugeri G, D'Amico AG, *et al*: Protective effects of PACAP in peripheral organs. Front Endocrinol (Lausanne) 11: 377, 2020.
16. D'Amico AG, Maugeri G, Saccone S, Federico C, Cavallaro S, Reglodi D and D'Agata V: PACAP modulates the autophagy process in an in vitro model of amyotrophic lateral sclerosis. Int J Mol Sci 21: 2943, 2020.
17. Lauretta G, Ravalli S, Szychlinska MA, Castorina A, Maugeri G, D'Amico AG, D'Agata V and Musumeci G: Current knowledge of pituitary adenylate cyclase activating polypeptide (PACAP) in articular cartilage. Histol Histopathol 35: 1251-1262, 2020.
18. D'Amico AG, Maugeri G, Musumeci G, Reglodi D and D'Agata V: PACAP and NAP: Effect of two functionally related peptides in diabetic retinopathy. J Mol Neurosci 71: 1525-1535, 2021.
19. Maugeri G, D'Amico AG, Musumeci G, Reglodi D and D'Agata V: Effects of pacap on schwann cells: Focus on nerve injury. Int J Mol Sci 21: 8233, 2020.
20. Castorina A, Scuderi S, D'Amico AG, Drago F and D'Agata V: PACAP and VIP increase the expression of myelin-related proteins in rat schwannoma cells: Involvement of PAC1/VPAC2 receptor-mediated activation of PI3K/Akt signaling pathways. Exp Cell Res 322: 108-121, 2014.
21. Maugeri G, D'Amico AG, Bucolo C and D'Agata V: Protective effect of PACAP-38 on retinal pigmented epithelium in an in vitro and in vivo model of diabetic retinopathy through EGFR-dependent mechanism. Peptides 119: 170108, 2019.
22. Vaudry D, Falluel-Morel A, Bourgault S, Basille M, Burel D, Wurtz O, Fournier A, Chow BK, Hashimoto H, Galas L and Vaudry H: Pituitary adenylate cyclase-activating polypeptide and its receptors: 20 years after the discovery. Pharmacol Rev 61: 283-357, 2009.
23. Zusev M and Gozes I: Differential regulation of activity-dependent neuroprotective protein in rat astrocytes by VIP and PACAP. Regul Pept 123: 33-41, 2004.
24. Dejda A, Sokołowska P and Nowak JZ: Neuroprotective potential of three neuropeptides PACAP, VIP and PHI. Pharmacol Rep 57: 307-320, 2005.
25. Lelievre V, Ghiani CA, Seksenyan A, Gressens P, de Vellis J and Waschek JA: Growth factor-dependent actions of PACAP on oligodendrocyte progenitor proliferation. Regul Pept 137: 58-66, 2006.
26. Bassan M, Zamostiano R, Davidson A, Pinhasov A, Giladi E, Perl O, Bassan H, Blat C, Gibney G, Glazner G, *et al*: Complete sequence of a novel protein containing a femtomolar-activity-dependent neuroprotective peptide. J Neurochem 72: 1283-1293, 1999.
27. Gozes I, Bassan M, Zamostiano R, Pinhasov A, Davidson A, Giladi E, Perl O, Glazner GW and Brenneman DE: A novel signaling molecule for neuropeptide action: Activity-dependent neuroprotective protein. Ann N Y Acad Sci 897: 125-135, 1999.

28. Zamostiano R, Pinhasov A, Gelber E, Steingart RA, Seroussi E, Giladi E, Bassan M, Wollman Y, Eyre HJ, Mulley JC, *et al*: Cloning and characterization of the human activity-dependent neuroprotective protein. J Biol Chem 276: 708-714, 2001.
29. Li M, David C, Kikuta T, Somogyvari-Vigh A and Arimura A: Signaling cascades involved in neuroprotection by subpicomolar pituitary adenylate cyclase-activating polypeptide 38. J Mol Neurosci 27: 91-105, 2005.
30. Nakamachi T, Li M, Shioda S and Arimura A: Signaling involved in pituitary adenylate cyclase-activating polypeptide-stimulated ADNP expression. Peptides 27: 1859-1864, 2006.
31. Nakamachi T, Ohtaki H, Yofu S, Dohi K, Watanabe J, Hayashi D, Matsuno R, Nonaka N, Itabashi K and Shioda S: Pituitary adenylate cyclase-activating polypeptide (PACAP) type 1 receptor (PAC1R) co-localizes with activity-dependent neuroprotective protein (ADNP) in the mouse brains. Regul Pept 145: 88-95, 2008.
32. Gozes I, Alcalay R, Giladi E, Pinhasov A, Furman S and Brenneman DE: NAP accelerates the performance of normal rats in the water maze. J Mol Neurosci 19: 167-170, 2002.
33. Pinhasov A, Mandel S, Torchinsky A, Giladi E, Pittel Z, Goldsweig AM, Servoss SJ, Brenneman DE and Gozes I: Activity-dependent neuroprotective protein: A novel gene essential for brain formation. Brain Res Dev Brain Res 144: 83-90, 2003.
34. Castorina A, Giunta S, Scuderi S and D'Agata V: Involvement of PACAP/ADNP signaling in the resistance to cell death in malignant peripheral nerve sheath tumor (MPNST) cells. J Mol Neurosci 48: 674-683, 2012.
35. Blaj C, Bringmann A, Schmidt EM, Urbischek M, Lamprecht S, Fröhlich T, Arnold GJ, Krebs S, Blum H, Hermeking H, *et al*: ADNP is a therapeutically inducible repressor of WNT signaling in colorectal cancer. Clin Cancer Res 23: 2769-2780, 2017.
36. Rangel R, Guzman-Rojas L, Kodama T, Kodama M, Newberg JY, Copeland NG and Jenkins NA: Identification of new tumor suppressor genes in triple-negative breast cancer. Cancer Res 77: 4089-4101, 2017.
37. Karagoz K, Mehta GA, Khella CA, Khanna P and Gatza ML: Integrative proteogenomic analyses of human tumours identifies ADNP as a novel oncogenic mediator of cell cycle progression in high-grade serous ovarian cancer with poor prognosis. EBioMedicine 50: 191-202, 2019.
38. Zhu S, Xu Z, Zeng Y, Long Y, Fan G, Ding Q, Wen Y, Cao J, Dai T, Han W and Xie Y: ADNP upregulation promotes bladder cancer cell proliferation via the AKT Pathway. Front Oncol 10: 491129, 2020.
39. Turashvili G: ADNP (Activity Dependent Neuroprotector Homeobox): A novel oncogene driving poor prognosis in high-grade serous carcinoma. EBioMedicine 51: 102589, 2020.
40. Gozes I, Morimoto BH, Tiong J, Fox A, Sutherland K, Dangoor D, Holser-Cochav M, Vered K, Newton P, Aisen PS, *et al*: NAP: Research and development of a peptide derived from activity-dependent neuroprotective protein (ADNP). CNS Drug Rev 11: 353-368, 2005.
41. Gozes I: Activity-dependent neuroprotective protein: From gene to drug candidate. Pharmacol Ther 114: 146-154, 2007.
42. Gozes I: NAP (davunetide) provides functional and structural neuroprotection. Curr Pharm Des 17: 1040-1044, 2011.
43. Maugeri G, D'Amico AG, Rasà DM, Saccone S, Federico C, Magro G, Cavallaro S and D'Agata V: Caffeine effect on HIFs/VEGF pathway in human glioblastoma cells exposed to hypoxia. Anticancer Agents Med Chem 18: 1432-1439, 2018.
44. Bonaventura G, Iemmolo R, D'Amico AG, La Cognata V, Costanzo E, Zappia M, D'Agata V, Conforti FL, Aronica E and Cavallaro S: PACAP and PAC1R are differentially expressed in motor cortex of amyotrophic lateral sclerosis patients and support survival of iPSC-derived motor neurons. J Cell Physiol 233: 3343-3351, 2018.
45. D'Agata V, Grimaldi M, Pascale A and Cavallaro S: Regional and cellular expression of the parkin gene in the rat cerebral cortex. Eur J Neurosci 12: 3583-3588, 2000.
46. Yao M, Li S, Wu X, Diao S, Zhang G, He H, Bian L and Lu Y: Cellular origin of glioblastoma and its implication in precision therapy. Cell Mol Immunol 15: 737-739, 2018.
47. Guichet PO, Guelfi S, Ripoll C, Teigell M, Sabourin JC, Bauchet L, Rigau V, Rothhut B and Hugnot JP: Asymmetric distribution of GFAP in glioma multipotent cells. PLoS One 11: e0151274, 2016.
48. Kim HJ, Park JW and Lee JH: Genetic architectures and cell-of-origin in glioblastoma. Front Oncol 10: 615400, 2020.
49. Belot N, Rorive S, Doyen I, Lefranc F, Bruyneel E, Dedecker R, Micik S, Brotchi J, Decaestecker C, Salmon I, *et al*: Molecular characterization of cell substratum attachments in human glial tumors relates to prognostic features. Glia 36: 375-390, 2001.
50. Bensalma S, Turpault S, Balandre AC, De Boisvilliers M, Gaillard A, Chadéneau C and Muller JM: PKA at a cross-road of signaling pathways involved in the regulation of glioblastoma migration and invasion by the neuropeptides VIP and PACAP. Cancers (Basel) 11: 123, 2019.
51. D'Amico AG, Scuderi S, Saccone S, Castorina A, Drago F and D'Agata V: Antiproliferative effects of PACAP and VIP in serum-starved glioma cells. J Mol Neurosci 51: 503-513, 2013.
52. Gozes I and Ivashko-Pachima Y: ADNP: In search for molecular mechanisms and innovative therapeutic strategies for frontotemporal degeneration. Front Aging Neurosci 7: 205, 2015.
53. Gozes I, Yeheskel A and Pasmanik-Chor M: Activity-dependent neuroprotective protein (ADNP): A case study for highly conserved chordata-specific genes shaping the brain and mutated in cancer. J Alzheimers Dis 45: 57-73, 2015.
54. Jo YS, Kim MS, Yoo NJ, Lee SH and Song SY: ADNP encoding a transcription factor interacting with BAF complexes exhibits frameshift mutations in gastric and colorectal cancers. Scand J Gastroenterol 51: 1269-1271, 2016.
55. Xie Y, Zhu S, Zang J, Wu G, Wen Y, Liang Y, Long Y, Guo W, Zang C, Hu X, *et al*: ADNP prompts the cisplatin-resistance of bladder cancer via TGF-β-mediated epithelial-mesenchymal transition (EMT) pathway. J Cancer 12: 5114-5124, 2021.
56. Scuderi S, D'Amico AG, Castorina A, Federico C, Marrazzo G, Drago F, Bucolo C and D'Agata V: Davunetide (NAP) protects the retina against early diabetic injury by reducing apoptotic death. J Mol Neurosci 54: 395-404, 2014.
57. D'Amico AG, Scuderi S, Maugeri G, Cavallaro S, Drago F and D'Agata V: NAP reduces murine microvascular endothelial cells proliferation induced by hyperglycemia. J Mol Neurosci 54: 405-413, 2014.
58. Bergers G and Benjamin LE: Tumorigenesis and the angiogenic switch. Nat Rev Cancer 3: 401-410, 2003.